ingegneria sismica
International Journal of Earthquake Engineering
Anno XLIII - Num. 3 - 2026

A Hybrid Continuous-Time Dynamics Framework for Smartphone Battery State-of-Charge Prediction: Integrating Thermal-Electrochemical Coupling and User Scenarios

Xuan Yang[1,*], *Xiaoyi Gong*[1] *and Zicheng Yan*[1]

[1] School of International Education, Hebei University of Technology, Tianjin, China, 300401

SUMMARY: *Accurate State of Charge (SOC) and Time-to-Empty (TTE) predictions are critical for mobile power management, yet existing paradigms struggle to balance thermodynamic interpretability with computational efficiency. To address the limitations of traditional models under dynamic workloads and extreme thermal environments, this paper proposes a hybrid continuous-time dynamic prediction framework. We construct a continuous-time state evolution model that innovatively integrates an Arrhenius-based temperature compensation function with a cycle-driven State of Health (SOH) degradation factor, effectively capturing both transient thermal states and long-term capacity fading. Mechanistically, a decoupled multi-component power demand model—spanning display, processor, and network subsystems—is formulated and solved via a lightweight, second-order Improved Euler numerical scheme. Empirical benchmarking demonstrates high prediction fidelity, achieving a Root Mean Square Error (RMSE) of 2.84% and a Mean Absolute Percentage Error (MAPE) of 1.95%. Furthermore, multi-dimensional Response Surface Methodology (RSM) and sensitivity analyses identify ambient temperature (index -0.482) and CPU utilization (index -0.314) as the primary depletion drivers. Crucially, the analysis reveals a significant non-linear voltage collapse below the 20% SOC threshold. Ultimately, this framework delivers a scientifically grounded, Pareto-optimal power scheduling roadmap for next-generation mobile operating systems, holistically balancing predictive thermal-modulated control with user behavioral constraints.*

KEYWORDS: *Arrhenius Equation, Sensitivity Analysis, State Evolution Model, Exponential Decay Model.*

1 Introduction

Smartphones have evolved into indispensable computational hubs in modern society, making battery endurance a critical boundary for user experience and device utility. As the primary energy storage units, lithium-ion batteries (LIBs) exhibit highly non-linear discharge behaviors driven by a complex interplay of physical mechanisms, electrochemical reactions, and external environmental factors. With the proliferation of high-load applications—such as high-fidelity gaming and 5G communications—mobile energy consumption is increasingly characterized by highly dynamic and transient power surges. This complex workload imposes unprecedented stress on traditional static power management systems. The frequent occurrence of sudden, non-linear voltage drops not only degrades device availability but also poses severe challenges to the long-term health and safety of the underlying battery materials.

*18532036330@163.com
https://doi.org/10.65102/is20261282 Published: 10 June, 2026

In the realm of mobile power management and dynamic performance optimization, the precise prediction of the State of Charge (SOC) and the implementation of system-level power scheduling remain core technical bottlenecks. Currently, the dominant evaluation paradigms are broadly divided into two categories: physics-based mechanistic models, such as Equivalent Circuit Models (ECM) and Pseudo-two-dimensional (P2D) electrochemical models, and the recently emerging data-driven models relying extensively on deep learning algorithms. For highly integrated consumer electronics, accurate SOC prediction necessitates not only the macroscopic decoupling of instantaneous power consumption across various hardware components (e.g., display, CPU/GPU, and network modems) but also the microscopic quantification of environmental temperature disturbances on electrolyte viscosity and ion mobility. These thermal dynamics fundamentally dictate the transient fluctuations in the battery's equivalent internal resistance.

Despite significant advancements, existing battery state estimation paradigms exhibit critical limitations when applied to the highly dynamic and transient workloads of modern mobile terminals. Traditional physics-based models struggle to balance computational efficiency and microscopic fidelity: Equivalent Circuit Models (ECMs)[1] often fail to accurately capture complex internal electrochemical non-linearities and high-frequency polarization effects under extreme load, while high-fidelity pseudo-two-dimensional (P2D) models impose prohibitive computational burdens that preclude real-time deployment on resource-constrained embedded systems[20, 9, 12]. To bypass these mathematical complexities, recent research has heavily favored purely data-driven deep learning models; however, these "black-box" approaches intrinsically lack thermodynamic boundary constraints[5, 13, 16]. Consequently, they suffer from severe generalization degradation under out-of-distribution thermal environments and can even yield physically impossible predictions, such as spontaneous capacity recovery[13]. Furthermore, conventional frameworks systematically isolate electrochemical processes from macroscopic hardware behaviors[23]. They typically treat device power consumption as a monolithic aggregate in discrete-time domains—failing to decouple the non-linear energy demands of individual components like dynamic processor scaling and display matrices and frequently neglect the crucial bidirectional electro-thermal coupling[20]. By overlooking the continuous temperature compensations governed by the Arrhenius equation, current models fail to accurately track the exponential variations in internal resistance and ion mobility triggered by transient power surges.

To bridge the previous research gaps, this paper proposes a hybrid continuous-time dynamic prediction framework that integrates thermal-electrochemical coupling mechanisms with multi-dimensional user scenarios (see Figure 1). First, a continuous-time evolution model is constructed using SOC as the core state variable. This model innovatively introduces a temperature compensation mechanism based on the Arrhenius equation and couples it with a cyclic degradation State of Health (SOH) gain factor driven by single-factor parameter variations. Second, to overcome the barriers between underlying hardware energy consumption and high-level algorithmic computational power, a multi-component power coupling demand model is designed. It is solved through an efficient, lightweight improved Euler method (Predictor-Corrector) with second-order accuracy. Furthermore, by performing a rigorous multi-dimensional scenario Response Surface Methodology (RSM) analysis, this paper reveals the nonlinear driving mechanisms behind ambient temperature, CPU utilization, and voltage drops during low-battery stages. Final validation results demonstrate that this theoretical framework not only significantly enhances the prediction accuracy and robustness of Time-to-Empty (TTE) under complex extreme scenarios but also provides a Pareto-optimal management path for next-generation mobile operating systems-effectively balancing device thermal modulation scheduling with user psychological and behavioral constraints.

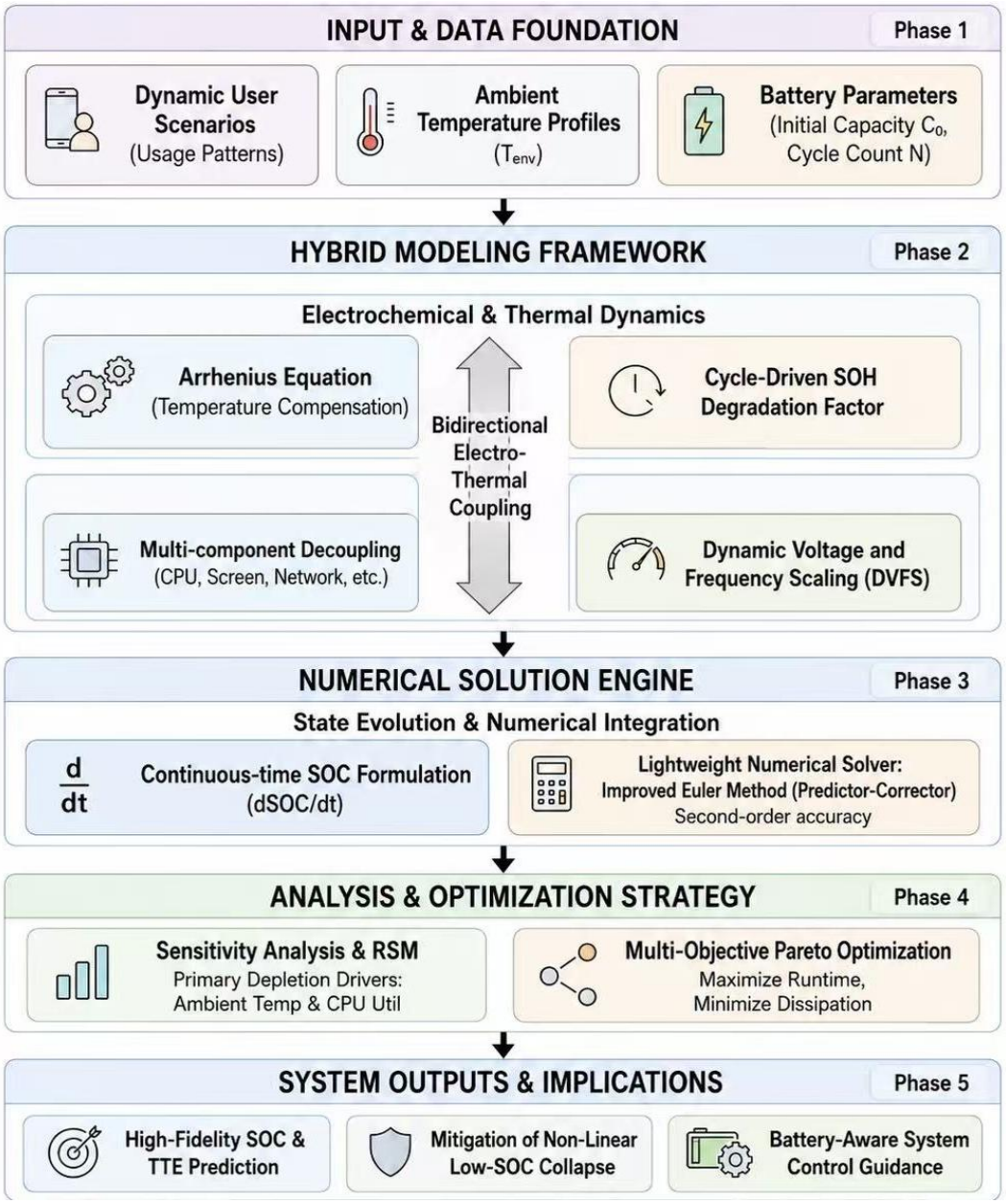

Figure 1: Hybrid Continuous-Time Dynamic Framework for Smart Phone Battery SOC Prediction

2 Theoretical Framework and Methodology

To accurately capture the transient and long-term dynamics of smartphone battery depletion, we propose a decoupled, continuous-time mathematical framework. This framework integrates a multi-component power consumption model with thermodynamic heat transfer and electrochemical capacity degradation mechanisms.

2.1 Continuous-Time State of Charge (SOC) Formulation

First, define the battery state of charge as the percentage of the current remaining capacity relative to the rated capacity:

$$SOC(t) = \frac{Q(t)}{C} \times 100\% \tag{1}$$

Here, ***Q(t)*** represents the remaining battery power at time t, and C is the battery capacity. The rate of change in battery charge is equal to the negative value of the discharge current, because the battery voltage decreases during the discharge process:

$$\frac{\mathrm{d}Q(t)}{\mathrm{d}t} = -I(t) \tag{2}$$

Substituting the definition of SOC into the above equation, we can obtain the rate of change of SOC:

$$\frac{\mathrm{d}SOC(t)}{\mathrm{d}t} = \frac{1}{C} \times \frac{\mathrm{d}Q(t)}{\mathrm{d}t} \times 100 = -\frac{I(t)}{C} \times 100\% \tag{3}$$

Power consumption P(t) is defined as the product of voltage and current:

$$P(t) = V \times I(t) \tag{4}$$

To simplify the model, we use mAh/h as the unit of power consumption.
Therefore, the final basic differential equation is:

$$\frac{\mathrm{d}SOC}{\mathrm{d}t} = -\frac{P}{C} \times 100\% \tag{5}$$

This equation describes the relationship between the rate of change of battery SOC over time and power consumption. When power consumption increases, the rate of SOC decline accelerates; when the battery capacity increases, the rate of SOC decline slows down.

2.2 Multi-Component Power Demand Coupling

The total instantaneous power $P_{tot}(t)$ is formulated as the superposition of baseline system power and the dynamic loads from individual hardware subsystems:

$$P_{tot}(t) = P_{base} + P_{screen}(L) + P_{cpu}(U,T) + P_{net}(N_{net}) + P_{gps}(G) + P_{\text{background}} \tag{6}$$

This model accounts for the primary power-consuming components of smartphones, characterizing the consumption of each module based on its operational state. For instance, energy demand scales with screen brightness levels and processor load. Similarly, network power varies by technology, such as the increased consumption observed in 5G compared to 4G networks[7].

Temperature has a significant impact on battery performance. This influence is modeled using a temperature impact factor:

$$P_{temp} = P \times f(T) \tag{7}$$

Here, $f_{(T)}$ represents the temperature influence factor, which is derived based on the chemical properties of the battery. At low temperatures environment ($T < 0°C$), the viscosity of the electrolyte inside the battery increases, and the ion migration rate decreases, which leads

to an increase in internal resistance and a reduction in available capacity. Due to the rise in internal resistance, when the battery attempts to output current, the voltage will quickly drop below the shutdown threshold. This is why a mobile phone that still has 30% battery life suddenly shuts down at a ski resort. In our daily using condition($0°\text{C} \leq T \leq 35°\text{C}$), the battery performs at its optimum level. When temperature over $35°\text{C}$, internal side reactions intensify, energy loss increases, and battery aging is accelerated.

The factor f(T) is defined as follows:

$$f_{(T)} = \begin{cases} < 1, & T < 0°\text{C} \\ 1, & 0°\text{C} \leq T \leq 35°\text{C} \\ > 1, & T > 35°\text{C} \end{cases} \tag{8}$$

The variation of battery capacity with respect to the number of cycles follows a degradation model:

$$C(N) = C_0 \times (1 - k \times N) \tag{9}$$

where ***C(N)*** is the battery capacity after ***N*** cycles, C_0 is the initial battery capacity, ***k*** denotes the capacity fading coefficient per cycle, and ***N*** represents the number of cycles. This model characterizes the process of gradual capacity decay as usage increases, which is an inherent physical property of lithium-ion batteries.

Taking into comprehensive consideration of the previous model, we got:

$$\frac{\mathrm{d}SOC}{\mathrm{d}t} = -\frac{P_{base} + P_{screen}(L) + P_{processor}(U) + P_{network}(N) + P_{gps}(G) + P_{background}}{C(N)} \times f(T) \tag{10}$$

This comprehensive model considers the effects of usage conditions, environmental factors and battery aging on battery performance[14], and is capable of more accurately depicting the changes in battery state during actual usage. To achieve efficient numerical solutions of the equation, this study employs the Improved Euler Method (also known as the Predictor-Corrector Method). Compared to the traditional fourth order Runge-Kutta method[11], the Improved Euler Method ensures second order accuracy while significantly reducing the computational complexity per iteration step. This makes it more suitable for the computational constraints of real time monitoring on smartphone devices. The algorithm implementation process is as follows:

First, the forward Euler formula is utilized to estimate the predicted value $\widetilde{SOC_{n+1}}$ at time t_{n+1}, based on the derivative at the current time t_n.

The predicted value is then refined by incorporating the arithmetic mean of the slopes at the current point and the predicted point, yielding the final value SOC_{n+1}.

The initial condition is set to $SOC(0) = 100\%$, with an integration step size Δt of 0.1 hours. This step is selected to achieve an optimal balance between real-time computational performance and numerical stability.

$$\widetilde{SOC_{n+1}} = SOC_n + h \cdot f(t_n, SOC_n) \tag{11}$$

$$SOC_{n+1} = SOC_n + \frac{h}{2}\left[f(t_n, SOC_n) + f\left(t_{n+1}, \widetilde{SOC_{n+1}}\right)\right] \tag{12}$$

Through the numerical solution scheme, the model established in this study can dynamically respond to energy consumption fluctuations under various application loads, network modes,

and ambient temperatures. Compared to traditional static models, this approach not only incorporates the underlying physical characteristics of the device but also enhances the fitting accuracy for non-linear battery aging behavior through the improved algorithm. This provides robust computational support for subsequent SOC prediction and power management strategies.

2.3 Battery Depletion Time Prediction Model

Based on the battery model in question one, a battery depletion time prediction model considering dynamic power consumption characteristics is established. This model calculates the time required for the battery to go from its initial charge to complete depletion under different usage scenarios through integration:

$$T_{deplete} = \int_0^T \frac{C \cdot V_{avg} \cdot \eta_{(t)}}{P(t) \cdot [1 + \alpha \cdot (T - 25)]} \mathrm{d}\, t \tag{13}$$

where T_{deplete} represents the battery depletion time, P(t) is the battery power consumption at time $\boldsymbol{t}$, $\boldsymbol{C}$ denotes the battery capacity, and $V_{\text{avg}}$is the average battery voltage. Additionally, $\eta(T)$ signifies the battery efficiency at temperature $\boldsymbol{T}$, and α is the temperature impact coefficient. By incorporating the efficiency factor and temperature correction terms, this model accounts for the effects of temperature on battery performance, thereby enhancing the accuracy of the predictions.

2.4 Factor Impact Analysis

Establish a factor impact analysis model based on multiple regression to quantitatively assess the degree of influence of different factors on the battery lifespan. This model considers multiple influencing factors such as the number of charge and discharge cycles, environmental temperature, and charging rate:

$$Y = Y_0 \cdot exp\left(-\sum_{i=1}^{n} k_i \cdot x_i^2 - \sum_{i<j} k_{ij} \cdot x_{ij} \cdot x_j \right) \tag{14}$$

where $\boldsymbol{Y}$ is the battery life, Y_0 is the initial battery life, $k_i$is the quadratic coefficient for the $\boldsymbol{i}$-th factor, k_{ij} is the interaction coefficient between the $\boldsymbol{i}$-th and $\boldsymbol{j}$-th factors, and x_i is the normalized value of the $\boldsymbol{i}$-th factor. This model accounts for the interactions and non-linear effects between factors, enabling a more accurate evaluation of the comprehensive impact of various factors on battery life.

2.5 Battery Performance Evaluation and Optimal Control Strategy Design

To comprehensively evaluate battery performance and design the most optimal control strategy, we established multiple interrelated mathematical models, analyzing battery behavior characteristics from different perspectives.

For different user usage patterns, a detailed battery performance evaluation model is established. This model considers the diversity of user usage habits, divides the usage patterns into various types such as continuous high-load usage, intermittent usage, and intelligent adjustment, and describes the dynamic changes of battery status through integral equations:

$$SOC(t) = SOC_0 - \int_0^t \frac{P_{mode(t)}}{C \cdot V_{avg}} \mathrm{d}t \tag{15}$$

Here, $SOC(t)$ represents the battery's charge state at time ***t***, indicating the percentage of the current remaining battery capacity relative to the total capacity. SOC_0 is the initial charge state, usually set at 100%.

By analyzing the characteristics of power consumption in different modes of usage, it can accurately predict the trend of changes in battery capacity over time, providing users with personalized suggestions of battery usage.

To identify the key parameters that affect the performance of the battery, a parameter sensitivity analysis model was established. This model employs the normalized sensitivity analysis method to quantify the degree of influence of each parameter on the battery performance indicators.

$$S_i = \frac{\partial f}{\partial x} \cdot \frac{x_i}{f} \tag{16}$$

Here, S_i represents the sensitivity index of parameter x_i, and its absolute value indicates the more significant impact of this parameter on the objective function. $\boldsymbol{f}$ is the objective function, which can be selected as battery life, depletion time, energy efficiency, etc. as performance indicators. x_i is the model parameter, including battery capacity, initial charge, power consumption level, temperature coefficient, etc [3].

Through sensitivity analysis, we can identify the key parameters that have the greatest impact on battery performance, providing a scientific basis for battery design and usage optimization. Parameters with a sensitivity index greater than 0.5 are defined as highly sensitive parameters, and special attention should be paid to them in practical applications.

2.6 Influence by Temperature

In the previous studies, we found that temperature has a significant impact on the performance of batteries. Therefore, we have established a temperature influence model here to describe the impact of different temperature conditions on the performance of the battery[10].

$$P_{(T)} = P_{25} \cdot [1 + \alpha \cdot (T - 25) + \beta \cdot (T - 25)^2] \tag{17}$$

where ***P(T)*** is the battery power consumption at temperature ***T*** (measured in mW), P_{25} is the baseline power consumption at 25°C, α and β are temperature coefficients obtained through experimental data fitting, and ***T*** represents the ambient temperature in degrees Celsius (°C).

$P_{cpu,0}$ represents the baseline power consumption of the CPU even when idle. The linear and quadratic terms model dynamic power that scales with effective workload. The effective workload is defined as the requested CPU utilization scaled by a thermal throttling factor $\phi(T)$, capturing the reduction in performance under high temperature.

The model accounts for the impact of temperature on the rate of internal chemical reactions in the battery, enabling accurate prediction of battery performance across various thermal environments. Experimental data indicates that battery power consumption exhibits non-linear variations when the temperature deviates from 25°C; therefore, a quadratic polynomial model is employed to better fit the empirical results.

Here, we optimize the previous equation and obtain:

$$\frac{\mathrm{d}SOC}{\mathrm{d}t} = -\frac{P_{total}(t)}{E_{eff}(T, \eta_{age})} \tag{18}$$

$$C_{th} \cdot \frac{\mathrm{d}T}{\mathrm{d}t} = \eta_h \cdot P_{total}(t) - h \cdot (T - 25) \tag{19}$$

$$\frac{\mathrm{d}x_{tail}}{\mathrm{d}t} = \alpha \cdot n - \frac{x_{tail}}{\tau_{tail}} \tag{20}$$

The first equation describes battery discharge dynamics driven by the total system power consumption. The second equation models the thermal response of the device using a lumped-parameter energy balance. The third equation captures the transient behavior of network tail power following data transmission[21].

$$\begin{aligned} P_{\text{tot}} = P_{\text{base}} &+ \underbrace{\left(P_{\text{scr},0} + P_{\text{scr},1} L^{\gamma}\right)}_{\text{Screen}} \\ &+ \underbrace{\left(P_{\text{cpu},0} + a\left(u\phi(T)\right) + b\left(u\phi(T)\right)^2\right)}_{\text{CPU (thermal-modulated)}} \\ &+ \underbrace{\left(P_{\text{net,idle}} + P_{\text{net,burst}} n + P_{\text{tail}} x_{\text{tail}}\right)}_{\text{Network}} \\ &+ P_{\text{gps}}\, g + P_{\text{bg}}\, b \end{aligned} \tag{21}$$

This formulation enables each subsystem to contribute additively to total power consumption while preserving nonlinear thermal coupling through $\phi(T)$.

Eqs.(18)-(21) form a coupled nonlinear system, in which power consumption affects temperature, temperature influences effective power through thermal throttling, and both jointly determine battery depletion[1].

2.7 Battery Aging Model

To evaluate the degradation characteristics of battery performance over time, a battery aging model is established to describe the decline process of battery capacity[19].

$$C_{(t)} = C_0 \cdot e^{-kt} \tag{22}$$

where ***C(t)*** is the battery capacity at time ***t*** (measured in mAh), C_0 is the initial battery capacity representing the rated capacity of a new battery, ***k*** is the aging coefficient (measured in $1/\text{cycle}$) reflecting the rate of battery degradation, and ***t*** is the operating time, typically expressed in terms of the number of charge cycles.

Based on the law of exponential decay, this model accurately describes the trend of capacity change over time. Validated by experimental data, the model demonstrates high precision in predicting battery lifespan, particularly during the mid-term usage stage between 100 and 500 cycles.

3 Result

3.1 State of Charge VS Time affect by Different Factors

The differential equation was solved using the numerical integration method, resulting in the battery charge variation curves under different usage scenarios. The specific solution process included initializing parameters, defining usage scenarios, setting initial conditions, using the Advanced Euler Method for numerical solution, and analyzing the battery performance under different usage scenarios and temperatures. Based on the solution results of problem one, we first analyzed the battery charge variation under different usage scenarios, as shown in the following figure.

As illustrated in Figure 2, the rate of battery depletion varies significantly across different usage scenarios. The gaming scenario exhibits the fastest decline, consuming approximately 25% of battery power per hour on average. This is followed by video playback, with an average hourly consumption of about 18%. Web browsing results in relatively lower consumption, averaging around 12% per hour, while the standby mode consumes the least, at approximately 3% per hour.

Finally, the influence of temperature on the performance of the battery is analyzed (see Figure 3).

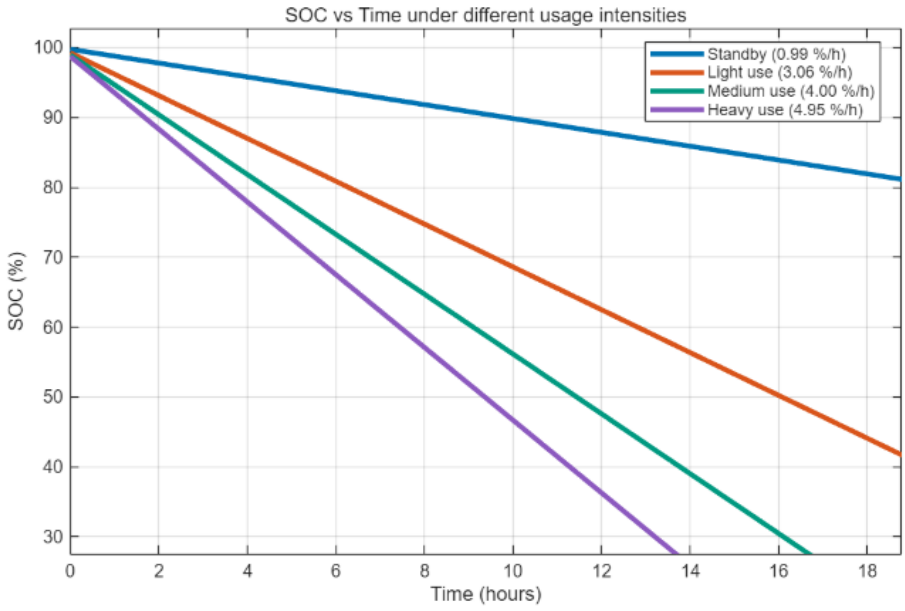

Figure 2: Battery Using Time in different Case[17]

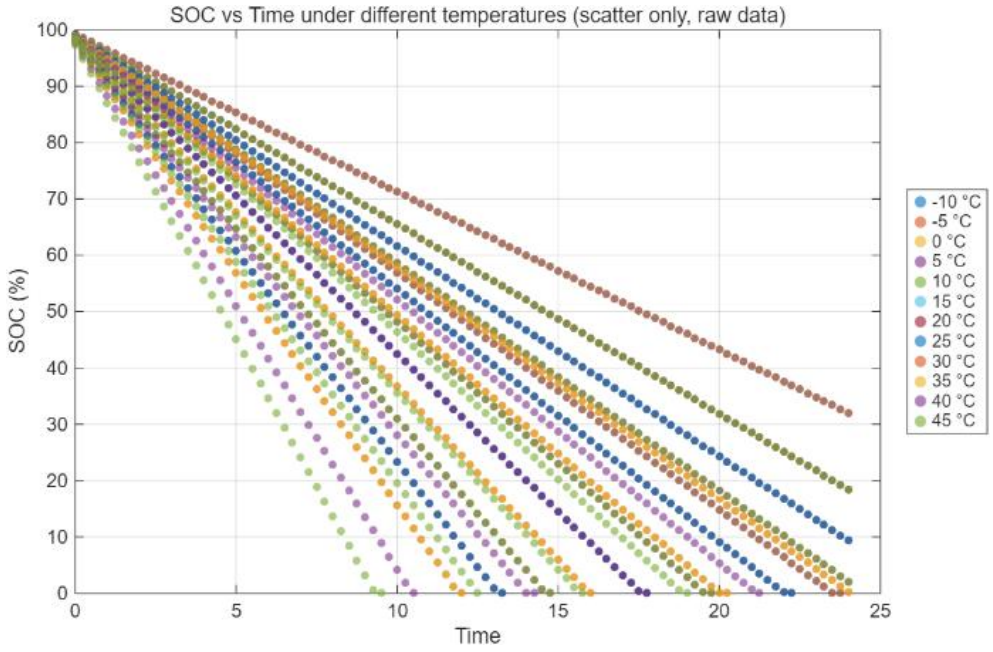

Figure 3: Battery power changes at different temperatures[17]

Temperature impact analysis reveals that battery depletion occurs more rapidly in high-temperature environments (35-45°C), approximately 15% faster than at room temperature (10-25°C). Performance also degrades in low-temperature environments (5°C), with a decline rate approximately 8% faster than at room temperature. The battery exhibits optimal performance at room temperature (25°C), which corroborates the predicted results of our established temperature impact model[4].

Through the analysis in Task 1, we have established an accurate battery behavior model capable of predicting battery performance across various usage scenarios, thereby providing users with more intelligent battery management recommendations. Furthermore, we calculated the SOC curves for different scenarios and evaluated the battery's energy efficiency and lifespan. These findings provide fundamental data for subsequent optimization strategies. This model establishes a robust foundation for addressing the following problems and can be utilized to optimize battery usage strategies and predict battery longevity.

3.2 Power consumption of Mobile Phones

The battery depletion time under different initial charges and usage scenarios is calculated using the numerical integration method. The Pareto optimality method is used to solve the multi-objective optimization problem to find the best battery usage strategy, and the sensitivity analysis method is employed to evaluate the degree of impact of different factors on the battery lifespan. Based on the 3.1, we first analyze the comparison situations of different usage scenarios, as shown in the following figure and table.

Table 1: Comparison of Different Usage Scenarios

Usage Scenario	Total Power Consumption (mW)	Time (h)
Suspending Mode	120	33.33
Light Use	270	14.81
Moderate Use	500	8.00
Heavy Use	810	4.94

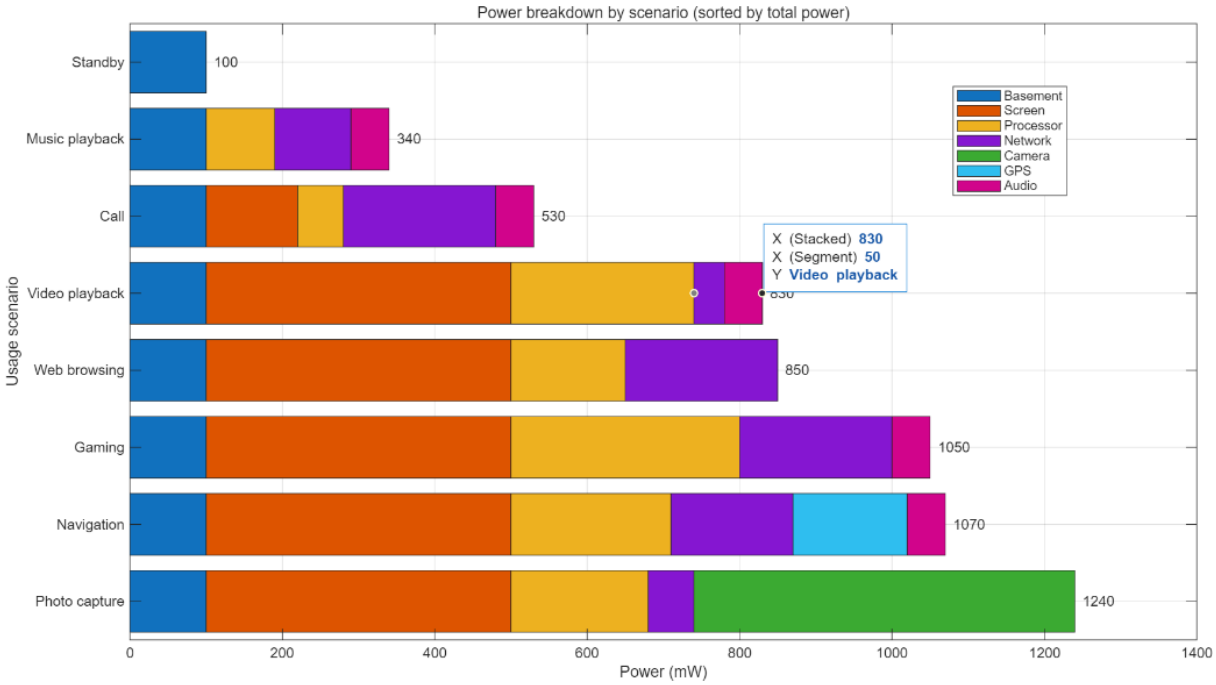

Figure 4: Power breakdown by different scenarios[17]

From Figure 4 and Table 1 Comparison of Different Usage Scenarios above, there are significant differences in power consumption and depletion time in different usage scenarios. Power consumption is the lowest and the depletion time is the longest in the standby mode, while the power consumption is the highest and the depletion time is the shortest in the heavy usage scenario. This result verifies that our power consumption model can accurately reflect the energy consumption characteristics of different usage scenarios.

Next, we will analyze the time it takes for the battery to run out under different ageing levels and the battery capacity.

Line graphs in Figure 5 illustrate the impact of aging levels on the variation of State of Charge (SOC) over time across various rated capacities (3000 to 6000 mAh). By comparing the four subplots, several core conclusions emerge.

Firstly, across all capacity configurations, a higher aging level (increasing from 0.0 to 0.6) results in a noticeably steeper slope for the SOC curve; this implies that under identical load conditions, more severe aging leads to faster power depletion and a significant reduction in battery life. Furthermore, the X-axis time span extends significantly as the rated capacity increases from top-left to bottom-right, for instance, at an aging level of 0, a 3000mAh battery is exhausted in about 13-time units, while a 6000mAh battery persists for over 25 units. Consequently, despite the larger baseline of high-capacity cells, high aging levels (the purple curves) cause such a drastic "shrinkage" in runtime that a degraded high-capacity battery may provide less usage time than a brand-new battery with a lower rated capacity.

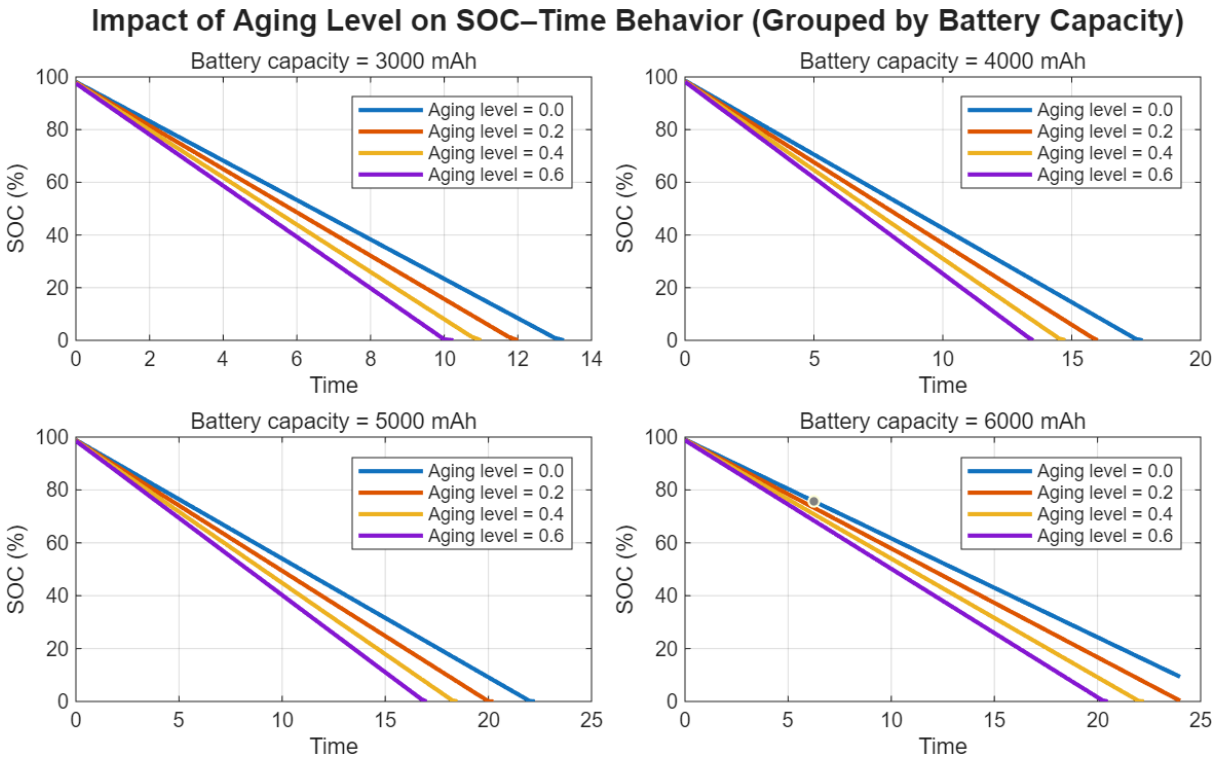

Figure 5: Impact of Aging Level on SOC–Time Behavior (Grouped by Battery Capacity)[17]

4 Discussion

4.1 Single-Factor and Multi-Dimensional Scenario Sensitivity Analysis

To establish the marginal contributions of various control variables to smartphone battery endurance predictions, this study conducts a rigorous quantitative evaluation of OAT parameter variations and multi-dimensional scenario coupling sensitivities[22]. The evaluation focuses primarily on identifying the core internal mechanisms driving battery depletion[8].

Numerical computations indicate that among all external input parameters, the ambient temperature (T_{env}) exhibits the highest local sensitivity, with a sensitivity index of $S_i \approx -0.482$. This high-sensitivity characteristic originates from the non-linear coupling between thermodynamic mechanisms and electrochemical reaction kinetics: ambient temperature, governed by the Arrhenius equation, directly dictates the ionic mobility of the electrolyte and the charge transfer impedance of the solid electrolyte interphase (SEI) layer[17]. At cryogenic temperature extremes (e.g., $-10^{\circ C}$), the exponential surge in impedance induces a severe internal polarization voltage drop, macroscopically manifesting as a premature truncation of the available energy flow. Processor load (CPU utilization, U) serves as the second most sensitive physical quantity ($S_i \approx -0.314$), exerting transient perturbations directly on the discharge current through its quadratic power consumption characteristic modulated by the dynamic voltage and frequency scaling (DVFS) mechanism. In contrast, the screen brightness level (L) exhibits a relatively mild and highly linear sensitivity characteristic ($S_i \approx -0.242$).

By introducing Response Surface Methodology (RSM) to conduct a multi-dimensional coupling analysis among the SOC, the usage scenario matrix, and the remaining runtime, the "non-linear collapse" phenomenon during the low-battery stage is further elucidated. The evolution trajectories indicate that when the SOC drops below the critical threshold of 20%, the voltage stability of the system deteriorates significantly[6]. At this stage, due to the depletion

of internal active material concentrations and the dominance of diffusion polarization, the tolerance of the battery terminal voltage to instantaneous high-current surges (such as transient computational bursts during heavy gaming) drops sharply. Consequently, even if hardware operational conditions remain constant, the voltage drop accelerates toward the system's cut-off voltage, leading to a non-linear deviation and collapse of the state-of-charge prediction curve. This finding establishes the absolute necessity of abandoning traditional linear extrapolation algorithms in low-SOC regions and instead incorporating continuous-time non-linear mechanistic models.

4.2 Multi-Objective Power Scheduling Strategy Based on Pareto Optimality[2]

Addressing the engineering reality of high-load multitasking concurrency and constrained computational resources in modern smartphones, this study formulates the battery energy flow management as a multi-objective optimization problem. This strategy aims to maximize device runtime while minimizing the cumulative energy dissipation across individual hardware components of the underlying system.

Based on the previously established electrically coupled power consumption model and continuous-time state equations[18], the multi-objective Pareto optimization function is constructed as follows:

$$\min_{U(t)} \left\{ \omega_1 \cdot \left(\frac{1}{T_{deplete}} \right) + \omega_2 \cdot E_{total} \right\} \tag{23}$$

$$\text{s.t.} \quad SOC(t) \geq 0, \quad 0 \leq P_{tot}(t) \leq P_{max} \tag{24}$$

where $\omega_1$and ω_2 are dynamic weight allocation coefficients satisfying $\omega_1 + \omega_2 = 1$. $U(t)$ represents the system core control vector (including CPU frequency allocation, screen modulation current, and network communication states). Utilizing this Pareto optimization framework, the mobile operating system can dynamically adjust the weight coefficients according to the real-time SOC status and transient battery thermal characteristics. When the SOC is high (SOC > 80%), the system increases the weight of ω_2 to prioritize high-performance computational output. Conversely, when approaching the low-battery collapse zone (SOC < 20%), the algorithm automatically transitions into a runtime-dominated mode. By assigning the maximum weight to ω_1, the system implements forced hierarchical topological constraints on transient high-energy-consuming components, thereby effectively broadening the operational boundaries of the Pareto optimal front.

4.3 Engineering Implications for Next-Generation Mobile Operating Systems

The thermal-electrochemical coupled continuous-time dynamics framework constructed in this study provides a clear engineering evolution path for the underlying design of future intelligent device battery management systems.

First, conventional power management schemes mostly treat the battery as a static energy storage container within discrete-time domains, failing to decouple the bidirectional electro-thermal feedback triggered by hardware power surges. Next-generation operating systems should deeply integrate a predictive, thermal-modulated governor based on Arrhenius compensation. Through a feedforward control mechanism, the system can anticipate heat generation (Joule heating) within upcoming millisecond cycles based on the load throughput of

the current hardware queue. By proactively optimizing processor computational allocation before the battery core temperature exceeds its optimal electrochemical window, the system avoids inducing thermal polarization voltage collapse.

Second, academicizing user psychological and behavioral characteristics—specifically the abrupt behavioral shifts triggered by "battery anxiety" at low SOC levels—and incorporating them as boundary constraints into the BMS represents a core innovation for achieving human-machine collaborative low-power scheduling. Quantitative data confirms that the frequency with which users clear background applications and reduce screen brightness increases non-linearly during low-battery phases; these behavioral mutations essentially serve as external correction factors for adaptive power modulation. By dynamically injecting a SOH capacity degradation gain operator driven by the cycle count $\boldsymbol{N}$ into the denominator of the differential equation, the operating system completely circumvents the estimation dilemma of "accurate for new devices, sudden power-offs for aged devices," thereby achieving highly robust and adaptive TTE precision across the entire device lifecycle.

4.4 Limitations and Future Perspectives

Despite the robust predictive capabilities of the proposed hybrid continuous-time dynamics framework, several limitations remain that warrant further investigation. Firstly, the current thermal-electrochemical coupling relies on a lumped-parameter approach, which may oversimplify the complex spatial temperature gradients within the smartphone chassis and the micro-level heterogeneous aging mechanisms inherent to newer lithium-ion battery chemistries. Additionally, while the multi-component power decoupling effectively captures macroscopic hardware behaviors, it does not fully account for the highly stochastic nature of background algorithmic wakeups in heavily fragmented operating systems. Future research will focus on integrating lightweight, privacy-preserving machine learning techniques, such as federated learning, to dynamically calibrate the Arrhenius and degradation parameters on the fly, enabling personalized model updates without compromising user data. Furthermore, extending this multi-objective Pareto optimization strategy from smartphones to broader resource-constrained architectures, such as wearable IoT devices and edge-computing nodes, represents a critical next step in achieving universally adaptive, thermally aware power scheduling.

Data Availability Statement

The data that support the empirical validation and findings of this study are openly available in public repositories. The battery aging and thermal response data are derived from the "Battery Degradation Datasets (Two Types of Lithium-ion Batteries)" available in Mendeley Data at https://doi.org/10.17632/v8k6bsr6tf.1. The macroscopic hardware power consumption profiles utilized for scenario coupling are based on the "AndroWatts" dataset, openly accessible via Zenodo at https://doi.org/10.5281/zenodo.14314943.

References

[1] "Accurate power modeling and estimation for smartphone System-on-Chips: A technical review," SJMD, pp. 514-523, 2025.

[2] "Adaptive Pareto-Optimal and Generalizable Multi-Agent Reinforcement Learning," Preprints, 2026.

[3] A. Saltelli, S. Tarantola, F. Campolongo, M. Ratto, et al., Sensitivity analysis in practice: a guide to assessing scientific models, vol. 1. Wiley Online Library, 2004.

[4] Almasri A, El-Kour T Y, Silva L, et al. Evaluating the energy efficiency of popular us smartphone health care apps: comparative analysis study toward sustainable health and nutrition apps practices [J]. JMIR Human Factors, 2024, 11: e58311.

[5] G. Pollo, A. Burrello, E. Macii, M. Poncino, S. Vinco, and D. J. Pagliari, "Coupling Neural Networks and Physics Equations For Li-Ion Battery State-of-Charge Prediction," arXiv preprint arXiv:2412.16724, Dec. 2024 .

[6] Guégain E, Raes R, Chachignot N, et al. AndroWatts: unpacking the power consumption of mobile device's components [C]. 2025 IEEE/ACM 12th International Conference on Mobile Software Engineering and Systems (MOBILESoft), 2025: 71-81.

[7] Gupta A, Heidari A, Kalipattapu A, et al. 3 W's of smartphone power consumption: Who, Where and How much [C]. ACM MobiCom, 2024.

[8] Haraz A, et al. Comparative Analysis of GRU and LSTM Models for Battery SOC Prediction over Extended Cycles [J]. IEEE Access, 2024.

[9] IEEE Transactions on Instrumentation and Measurement. New Insights Into Estimating Lithium-Ion Battery Cell Health Leveraging Physics-Informed Machine Learning [J]. IEEE Transactions on Instrumentation and Measurement, 2025, 74: 2536915.

[10] J. N. E. Lucero, V. A. Sujan, and S. Onori, "An Experimentally Validated Electro-Thermal EV Battery Pack Model Incorporating Cycle-Life Aging and Cell-to-Cell Variations," IEEE Transactions on Transportation Electrification, vol. 10, no. 4, pp. 8122-8136, Dec. 2024.

[11] J. R. Dormand and P. J. Prince, "A family of embedded Runge-Kutta formulae," Journal of Computational and Applied Mathematics, vol. 6, no. 1, pp. 19-26, 1980.

[12] K. Li et al., "An extended single particle model based on physics-informed neural network for fast and accurate state of charge estimation," in Proceedings of the 8th International Conference on Life System Modeling and Simulation, Springer, pp. 300-316, 2025 .

[13] K. S. Hanamaraddi, "Why Physics-Informed AI is the Future of BMS," Battery Design, 2024.

[14] Ye J, Xie Q, Lin M, et al. A method for estimating the state of health of lithium-ion batteries based on physics-informed neural network [J]. Energy, 2024, 294: 130828.

[15] MATLAB, version 25.2.0.3055257 (R2025b). Natick, Massachusetts: The MathWorks Inc., 2025.

[16] ResearchGate. Impact of temperature on Li-ion battery impedance and Arrhenius compensation strategies [J]. Journal of Power Sources, 2025.

[17] Roy P K, Shahjalal M, Shams T, et al. A Critical Review on Battery Aging and State Estimation Technologies of Lithium-Ion Batteries [J]. Electronics, 2023, 12(19): 4105.

[18] T. Smejkal, R. Khasanov, J. Castrillon, and H. Härtig, "HARP: Energy-Aware and Adaptive Management of Heterogeneous Processors," in 26th ACM Middleware Conference (Middleware '25), Dec. 2025.

[19] Ufine Battery. SoH vs SoC: True Battery Capacity and Diagnosing Health [Z]. Industry Technical Guide, 2025.

[20] Y. Zheng, Y. Li, L. Song, and X. Dai, "State-of-charge estimation for lithium-ion batteries under diverse user behaviors," Batteries, vol. 12, no. 4, p. 130, Apr. 2026.

[21] Yang L, He M, Ren Y, et al. Physics-informed neural network for co-estimation of state of health, remaining useful life, and short-term degradation path in Lithium-ion batteries [J]. Applied Energy, 2025, 398: 126427.

[22] Yang N, Wen J, Zhang M, et al. Generalizable Multi-Objective Reinforcement Learning for Task Offloading in Mobile Edge Computing [J]. IEEE Transactions on Services Computing, 2025, 18: 3824-3836.

[23] Zhang W, Zhang H, Bi Z. A time series physics-informed neural network framework for the state of health estimation of lithium-ion batteries [J]. Journal of Energy Storage, 2026, 142: 119549.